Loss of ZMPSTE24 (FACE-1) causes autosomal recessive restrictive dermopathy and accumulation of Lamin A precursors

Claire L. Navarro, Juan Cadiñanos, Annachiara de Sandre-Giovannoli, Rafaelle Bernard, Sebastien Courrier, Irène Boccaccio, Amandine Boyer, Wim J Kleijer, Anja Wagner, Fabienne Giuliano, et al.

Loss of ZMPSTE24 (FACE-1) causes autosomal recessive restrictive dermopathy and accumulation of Lamin A precursors

Claire L. Navarro[1], Juan Cadiñanos[2], Annachiara De Sandre-Giovannoli[3], Rafaëlle Bernard[3], Sébastien Courrier[4], Irène Boccaccio[1], Amandine Boyer[3], Wim J. Kleijer[5], Anja Wagner[5], Fabienne Giuliano[6], Frits A. Beemer[7], Jose M. Freije[2], Pierre Cau[1], Raoul C.M. Hennekam[8], Carlos López-Otín[2], Catherine Badens[3,4] and Nicolas Lévy[1,3,4,*]

[1]Inserm U491, Faculté de Médecine de Marseille, Marseille, France, [2]Departamento de Bioquimica y Biologia Molecular, Instituto Universitario de Oncologia, Universidad de Oviedo, Spain, [3]Département de Génétique Médicale, Hôpital d'enfants de la Timone, Marseille, France, [4]Centre d'Enseignement et de Recherche en Génétique Médicale, Faculté de médecine, Marseille, France, [5]Clinical Genetics, Erasmus Medical Center, Rotterdam, The Netherlands, [6]Service de Génétique Médicale, CHU Nice, Hôpital de l'Archet, Nice, France, [7]Clinical Genetics Center, University Medical Center, Utrecht, The Netherlands and [8]Department of Pediatrics and Clinical Genetics, Academic Medical Center, Amsterdam, The Netherlands

UCSC/GenBank accession nos CA881610, X03444.1 and Y13834

Restrictive dermopathy (RD) is characterized by intrauterine growth retardation, tight and rigid skin with prominent superficial vessels, bone mineralization defects, dysplastic clavicles, arthrogryposis and early neonatal death. In two patients affected with RD, we recently reported two different heterozygous splicing mutations in the *LMNA* gene, leading to the production and accumulation of truncated Prelamin A. In other patients, a single nucleotide insertion was identified in *ZMPSTE24.* This variation is located in a homopolymeric repeat of thymines and introduces a premature termination codon. *ZMPSTE24* encodes an endoprotease essential for the post-translational cleavage of the Lamin A precursor and the production of mature Lamin A. However, the autosomal recessive inheritance of RD suggested that a further molecular defect was present either in the second *ZMPSTE24* allele or in another gene involved in Lamin A processing. Here, we report new findings in RD linked to *ZMPSTE24* mutations. Ten RD patients were analyzed including seven from a previous series and three novel patients. All were found to be either homozygous or compound heterozygous for *ZMPSTE24* mutations. We report three novel 'null' mutations as well as the recurrent thymine insertion. In all cases, we find a complete absence of both ZMPSTE24 and mature Lamin A associated with Prelamin A accumulation. Thus, RD is either a primary or a secondary laminopathy, caused by dominant *de novo LMNA* mutations or, more frequently, recessive null *ZMPSTE24* mutations, most of which lie in a mutation hotspot within exon 9. The accumulation of truncated or normal length Prelamin A is, therefore, a shared pathophysiological feature in recessive and dominant RD. These findings have an important impact on our knowledge of the pathophysiology in Progeria and related disorders and will help direct the development of therapeutic approaches.

*To whom correspondence should be addressed at: Inserm U491: 'Génétique Médicale et Développement', Faculté de Médecine de Marseille, 13385 Marseille Cedex 05, France. Tel: +33 491786894; Fax: +33 491804319; Email: nicolas.levy@medecine.univ-mrs.fr

INTRODUCTION

Restrictive dermopathy (RD), first described by Witt *et al.* (1), is a lethal neonatal genodermatosis (MIM no. 275210) in which tautness of the skin causes fetal akinesia or hypokinesia deformation sequence. Reduced fetal movements or fetal immobility precede premature delivery and neonatal death. Other manifestations include a tightly adherent, thin, translucent skin with prominent vessels, characteristic facial features, generalized joint contractures, enlarged fontanels, dysplasia of clavicles, respiratory insufficiency and an enlarged placenta with short umbilical cord (2–4). Skin abnormalities are often visible histologically and include thin dermis, abnormally dense collagen bundles, although the elastic fibres are almost completely absent.

Recently, prompted by the similarities in clinical features between RD and Progeria, we checked RD patients for mutations in *LMNA*, because the G608G mutation in *LMNA* is the major cause of Progeria (5,6). In this previous study, two RD patients harboured truncating splice mutations in *LMNA* exon 11 leading to the production of truncated Lamin A precursors, whereas the other seven patients carried *LMNA* wild-type alleles (7). These latter cases were further screened for mutations in *ZMPSTE24*, also called *FACE-1* in human, which is responsible for Lamin A processing (8–11). A single heterozygous insertion was found in *ZMPSTE24* exon 9 for all seven patients. Although this did not fully explain the autosomal recessive inheritance in RD families (7), subsequent functional explorations including western blot and immunocytochemistry provided evidence for the absence of mature Lamin A and presence of normal Lamin C together with major nuclear disorganization. In addition, nucleoplasmic foci stained with anti-Lamin A antibodies indicated an accumulation of Prelamin A.

Lamins A and C, the major isoforms of A-type lamins, are expressed in all vertebrate differentiated cells (12) and are translated from alternatively spliced transcripts of the *LMNA* gene. A- and B-type lamins assemble to form the nuclear lamina, a filamentous meshwork forming an interface between the inner nuclear membrane and the chromatin (13). Lamins A and C are also located throughout the nucleoplasm (14,15), where they seem to play fundamental roles in DNA replication and RNA transcription (reviewed in 16). Mature Lamin A isoforms are processed through a series of post-translational modifications performed on the Prelamin A precursor. The modifications of Prelamin A include, successively, farnesylation of the cysteine in the C-terminal CaaX motif (C, cysteine; a, aliphatic; X, any amino acid), followed by a proteolytic cleavage of the aaX-terminal tripeptide (amino acids 662–664), methylation of the prenylated cysteine and a second cleavage of the remaining 15 C-terminal residues (amino acids 647–661) (11,17,18). The enzyme responsible for these sequential proteolytic cleavages is the zinc metalloproteinase ZMPSTE24 for which Lamin A is the only known substrate in mammals (11). Skeletal abnormalities and lipodystrophy have been reported in mice inactivated for *Zmpste24* (9,10) and it has been demonstrated that decreasing the level of Prelamin A synthesis, corrects the progeroid phenotype observed in *Zmpste24*−/− mice (19). Mutations in human *ZMPSTE24* have been identified in patients affected with mandibuloacral dysplasia (MAD) (20) and RD (7). It is noteworthy that, regardless of the associated phenotype, *ZMPSTE24* mutations are recessive and all reported patients carry a common allele, consisting of a single thymine (T) insertion in a T repeat at exon 9 (7,20). In MAD, the second associated allele carries a missense substitution that is presumed to result in the production of a partially functional protein (20).

In contrast to *LMNA* mutations, which have been identified in at least 10 distinct disorders involving different tissues, singly or in combination (striated muscle, peripheral nerve, adipose tissue, bone and skin) (21,22), *ZMPSTE24* defects are associated with phenotypes that mainly show features similar to Hutchinson–Gilford progeria syndrome (HGPS) and belong to the spectrum of *LMNA*-associated diseases because they affect the Lamin A C-terminal globular domain (reviewed in 22,23).

Here, we report our molecular and functional exploration of ten patients affected with autosomal recessive RD (AR-RD). Seven patients were included from our previous study whereas three have been collected recently. Our results indicate that AR-RD is caused by defects in ZMPSTE24 with all patients being either homozygous or compound heterozygous. In all cases explored, we demonstrate that the absence of both ZMPSTE24 and mature Lamin A proteins as well as the presence of normal length unprocessed Lamin A precursors. Our immunocytochemical studies indicate that Prelamin A accumulates within the nucleoplasm, co-localizing with Emerin but not with Lamin B1.

RESULTS

Ten patients from nine families are reported in this series, seven of them have been previously described (P3–P9), whereas three have been recently recruited at our genetics center (P10–P12). Phenotypes were clinically homogeneous among patients and have been detailed in previous studies (7,24,25). In brief, patients were born to healthy non-consanguineous parents and showed typical RD signs both during pregnancy and at birth including reduced fetal movements, severe intra uterine growth retardation and pre-term delivery. A family history was reported in three families although only patients P5 and P6 from this study belonged to the same sibship.

In our previous study, a common single mutation in *ZMPSTE24* (c.1085_1086InsT) was characterized in seven RD patients. The three more recent patients (P10, P11 and P12) were found to carry the same insertion. In order to determine whether another mutant allele of *ZMPSTE24* was present or if the hypothesis of digenic inheritance of mutations in *ZMPSTE24* and another gene could be demonstrated, we first searched for the presence of ZMPSTE24 protein in RD fibroblasts or tissue samples from six different RD patients (P3, P5, P7, P9, P10 and P11). ZMPSTE24 protein was absent in AR-RD patients' cells whereas it was observed in controls: normal cells and cells from Progeria or RD patients carrying the *LMNA*-G608G mutation (Fig.1A). To complete and confirm these results, antibodies against Lamins A/C were used on the same western blot and showed not only

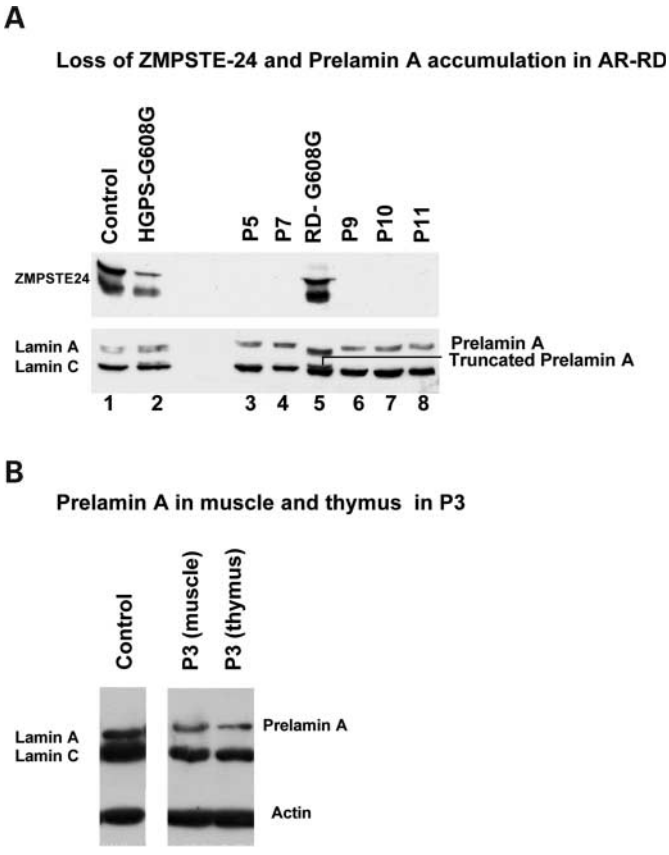

Figure 1. Western blot analysis of ZMPSTE24 and Lamin A/C in patients affected with RD. (**A**) Loss of ZMPSTE24 and Prelamin A accumulation in AR-RD patients. Lane 1: normal control fibroblasts; lanes 2 and 5: fibroblasts from LMNA-G608G patients presenting either typical HGPS or RD; lanes 3, 4, 6, 7 and 8: fibroblasts from AR-RD patients. Loss of ZMPSTE24 protein is shown for all AR-RD patients when compared with normal or *LMNA*-G608G fibroblasts used as controls. Prelamin A is present in all patients, in association with the complete absence of both ZMPSTE24 and mature Lamin A proteins. In lanes 2 and 5, truncated Prelamin A is observed as the G608G mutation mediates the activation of a cryptic site in *LMNA* and leads to a 50 amino acid deletion in Prelamin A. Lamin A is only present in normal and G608G controls, whereas Lamin C is unaffected in AR-RD patients and controls. (**B**) Prelamin A accumulation in muscle and thymus from patient P3.

the lack of normal mature Lamin A as previously reported but also a strong signal corresponding to normal length Prelamin A in all patients explored (Fig. 1A and B). This suggested that the loss of ZMPSTE24 protein was a consequence of the presence of null homozygous or compound heterozygous mutations in *ZMPSTE24*, preventing the synthesis of either a normal or an aberrant polypeptide.

We, therefore, focused the mutation search on *ZMPSTE24*. As no other anomaly except that in exon 9 was identified either at the genomic level or after RT–PCR experiments performed to amplify short overlapping cDNA fragments, half to full-length cDNAs were generated using different primer combinations and sequenced. This procedure allowed us to identify novel mutations in *ZMPSTE24*. In patient P4, a shorter fragment suggestive of a large intragenic deletion was evidenced. Indeed, all patients presented the normal length fragment, although an extra shorter band was observed for patient P4 with different primer pairs (Fig. 2A). Sequencing of this fragment revealed an abnormal cDNA containing a direct junction between exons 2 and 6 removing 357 nucleotides (nt) at the mRNA level (r.271_627del) (Fig. 2A). At the protein level, this deletion was predicted to remove all of the 119 amino acids encoded by exons 3, 4 and 5 (p.Leu91_Leu209del). To determine the corresponding genomic deletion, long-range PCR experiments were performed on DNAs from the patient and his parents with a set of primers selected in introns 2 and 6, respectively. This allowed us to amplify a specific junction fragment, to evaluate the deletion's size, to further characterize its breakpoints and to determine its parental inheritance (Fig. 2B). The genomic deletion extends from nt 40684 to 46112 of GenBank accession no. AL050341.18. It spans 5428 bp between proximal and distal breakpoints located in introns 2 and 5, respectively (Fig. 2C). Patient P4 is thus compound heterozygous for the c.1085_1086insT in exon 9 and a large deletion (r.271_627del, at the RNA level) on the opposite allele. The analysis of parental DNAs indicated that this deletion was maternally inherited (Fig. 2B).

In a second patient (P10), sequencing of the full-length cDNA revealed a C > T transition at nt 1249 (c.1249C > T) which was confirmed at the genomic level (Fig. 2D). This transition predicts a nonsense substitution from glutamine to stop in exon 10 (p.Gln417X).

In patient P12, genomic analysis evidenced a cytosine deletion (c.295delC) in exon 3 leading to a shifted reading frame and the creation of a premature termination codon (PTC), appearing 38 codons after the insertion (p.Pro99LeufsX38) (Fig. 2E). No further studies could be performed from this patient as only DNA was available.

These results obtained from three patients, two of them have been recently collected (P10, P12), confirmed that a second mutation was to be searched for in *ZMPSTE24* in the other seven RD patients, rather than in another gene. All the patients identified to date with *ZMPSTE24* mutations carry a common thymine insertion in a homopolymeric tract in exon 9 (c.1085_1086insT). We, thus, hypothesized that a mutation could lie within the same T stretch on the other *ZMPSTE24* allele. As we now had DNA available from both parents in some of these families, PCR fragments encompassing exon 9 were generated for each patient and available parent and directly sequenced. This indicated that, in four families, each parent was heterozygous for c.1085_1086insT, making it very likely that their affected child was homozygous for this mutation. However, repeating the sequencing of exon 9 in these affected probands indicated a frameshift pattern, although it was less pronounced when compared with heterozygous parents (Fig. 3A). A genomic instability of the homopolymeric thymine tract was suspected and the corresponding PCR fragments were subcloned in the pGEM-T vector before sequencing by SP6 or T7 primers. This demonstrated that seven patients previously evaluated as heterozygous, were in fact homozygous for the c.1085_1086InsT [(T)10 instead of (T)9 in wild-type]. Interestingly, we obtained clones that included an aberrant number of thymines in the repeat, although high fidelity Taq polymerase was used. Seventeen out of 145 (11%) clones from homozygous and heterozygous individuals, carried either an aberrant number of thymines in

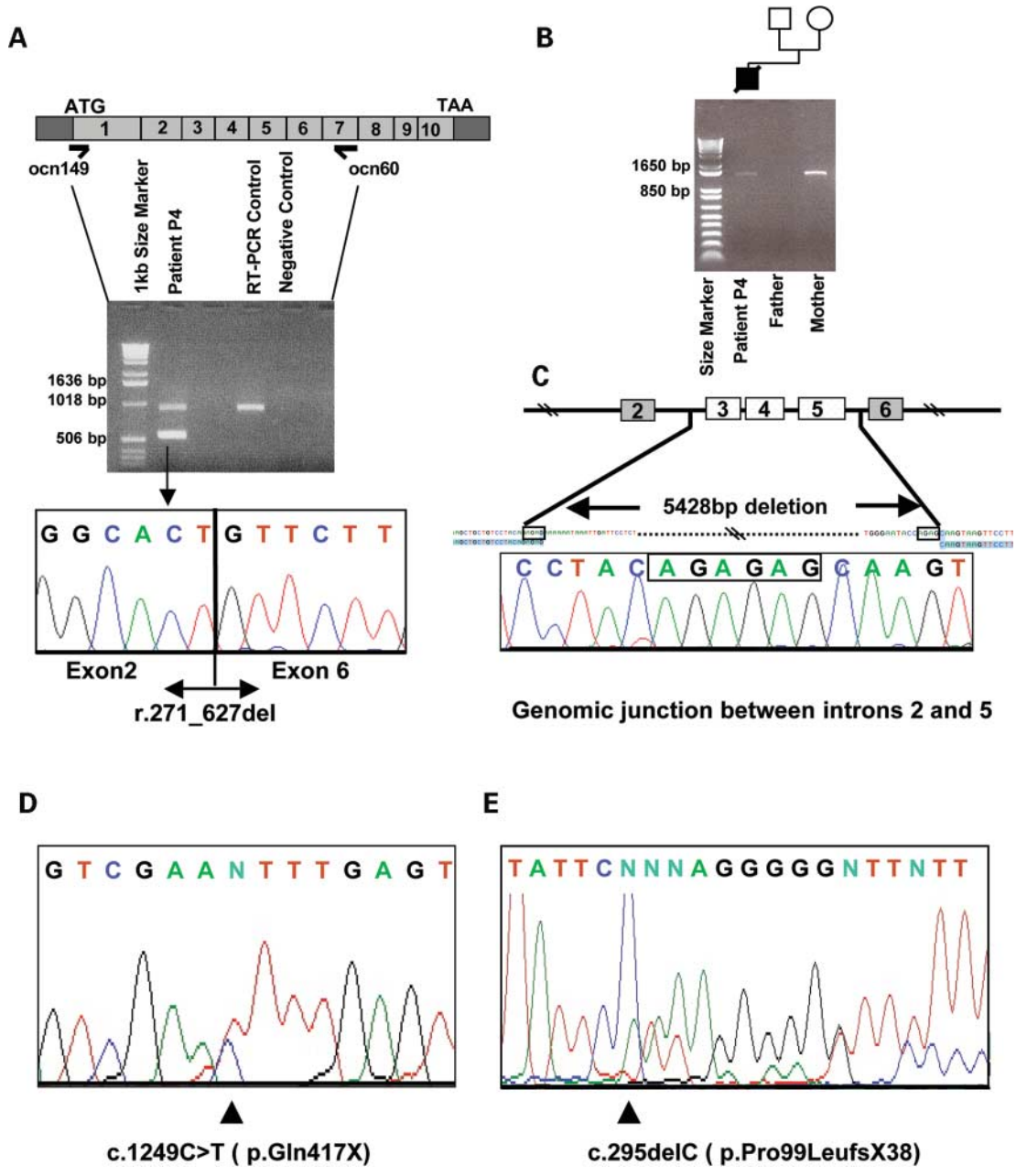

Figure 2. *ZMPSTE24* mutations in AR-RD patients P4, P10 and P12. These mutations represent the second mutation in ZMPSTE24 as these patients share a c.1085_1086insT in the other allele (see text and Fig. 3). (**A**) Analysis of *ZMPSTE24* transcripts in patient P4. Control and patient cDNAs amplified by RT–PCR using primers ocn149 (forward in exon 1) and ocn60 (reverse in exon 7) produced a normal sized PCR product (902 bp) whereas an extra shorter band (545 bp) was obtained in samples from the patient. The shorter band was sequenced (arrow) and revealed a direct and aberrant junction between exons 2 and 6, corresponding to a 357 nt deletion in the mRNA (r.271_627del) and the in-frame skipping of exons 3, 4 and 5. (**B**) *ZMPSTE24* genomic analysis in patient P4. PCR amplified fragments from genomic DNA of patient P4 (black square), and his parents, using primers int2F2 (forward in intron 2) and ocn48 (reverse in intron 6). A specific 1.388 kb size fragment is amplified from P4 and his mother, showing that the 5.428 kb deletion had been maternally inherited. Under the PCR conditions used, the expected wild-type fragment of 6.816 kb is not detected. (**C**) Schematic representation of the genomic deletion in P4. Light grey boxes indicate the deleted exons 3, 4 and 5 and the dark grey boxes represent the exons 2 and 6, maintained in the deleted allele. Upper sequence represents the genomic reference sequence, and the lower sequence (highlighted in blue) is the deleted sequence. The electropherogram corresponds to the genomic junction fragment and the breakpoints, lying in AG dinucleotide repeats, are boxed. (**D**) c.1249C>T mutation (p.Gln417X) in *ZMPSTE24* exon 10 in patient P10. (**E**) c.295delC mutation (p.Pro99LeufsX38) in *ZMPSTE24* exon 3 from patient P12. Note the frameshift pattern after the cytosine deletion.

the repeat [(T)8, (T)11 and (T)12] or a wild-type sequence [(T)9] from homozygous patients (Supplementary Material, Fig. S1). This result strongly suggested an homopolymeric instability, thus corroborating the direct sequencing results.

To confirm the sequencing experiments, fluorescent PCR fragments encompassing the mutation were generated (Fig. 3A). This method does not detect the low number of aberrant DNA molecules generated from the instability and

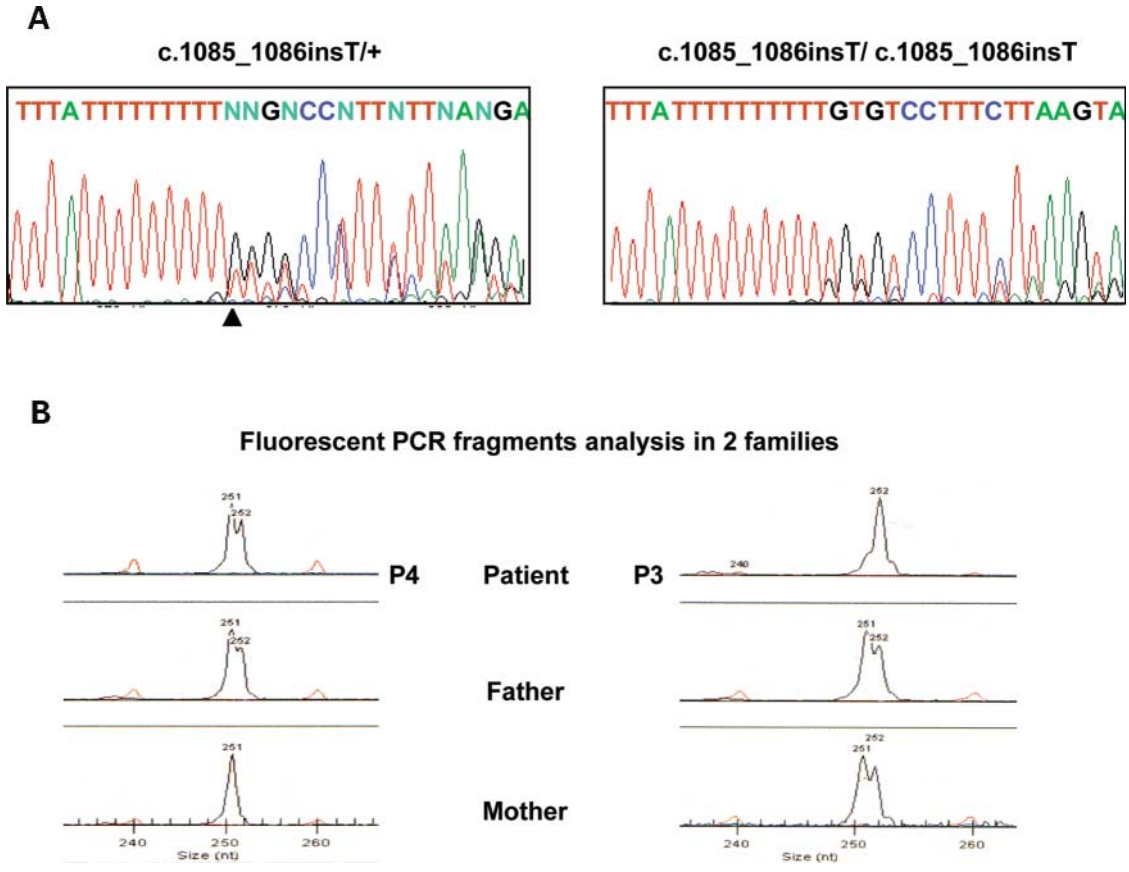

Figure 3. Molecular analysis of the c.1085_1086InsT mutation (L362fsX18). (**A**) Direct sequencing of PCR products generated using DNA from a heterozygous carrier (left panel) and from a homozygous patient (right panel). (**B**) Fluorescent PCR analysis of fragments encompassing exon 9, in DNA from two unrelated patients. A 1 bp difference between the wild-type (T)9 and mutant (T)10 alleles is evident and correlates with the mutation status in all families. Left panel: patient P4 is heterozygous (251/252 bp) for the thymine insertion which is paternally inherited. His mother is homozygous for the wild-type allele (251/251). Right panel: segregation analysis for a homozygous patient who received the thymine insertion from both of his heterozygous parents.

generated specific peaks for the (T)9 and (T)10 alleles. These results were perfectly consistent with the sequencing analysis and confirmed the homozygous or heterozygous status for the c.1085_1086InsT mutation in all the individuals explored in this study. Overall, the c.1085_1086InsT mutation has been found in 17 out of 20 chromosomes explored from the *ZMPSTE24*-mutated RD patients (P3–P12).

In silico protein predictions were performed to evaluate the potential effect of *ZMPSTE24* mutations identified in this study. It is important to point out that all of the mutations identified, that we were able to explore at the transcriptional level, did not alter mRNA expression (Fig. 2A and data not shown) and were thus predicted to direct the translation of a truncated and/or mislocalized protein (Fig. 4). However, although ZMPSTE 24 is never observed in patient's cells, we hypothesize that it is either not translated or degraded after translation.

Immunocytochemical explorations were performed on patients' fibroblasts, using antibodies directed against Lamins A/C, Lamin A, Lamin B1 and Emerin. As a complete loss of Lamin A was observed, anti-Lamin A antibody was used to detect Prelamin A, in AR-RD patients.

Double labelling was performed using different antibody combinations (anti-Lamin A/C with anti-Lamin A, anti-Lamin A/C with anti-Lamin B1, anti-Lamin B1 with anti-Emerin). Numerous and major nuclear deformities were observed (Fig. 5). Blebs or herniations were present and shown to specifically contain Lamin C and Emerin but not Lamin A and B1. Nuclear blebs (Fig. 5A–C) were labelled with anti-Lamin A/C but not anti-Lamin A antibodies (Fig. 5A and C). Nucleoplasmic aggregates were observed with anti-Lamins A/C, anti-Lamin A (Fig. 5B) and anti-Emerin but not anti-Lamin B1 (Fig. 5C and D). At the nuclear rim, fluorescent labelling corresponding to Lamin A, Lamin A/C and Emerin was clearly reduced and, in some nuclei, a honeycomb structure was observed with anti-Lamin A/C whereas no staining was present for anti-Lamin B1 (Fig. 5D and E).

DISCUSSION

Recently, we reported that RD was genetically heterogeneous, either caused by heterozygous *de novo* splicing mutations specifically affecting *LMNA* exon 11 and leading to the synthesis of truncated Prelamin A (7) or, more frequently, associated with a null mutation in *ZMPSTE24* and loss of mature Lamin A synthesis (7). In both cases, dramatic nuclear damage with nucleoplasmic accumulation of unprocessed

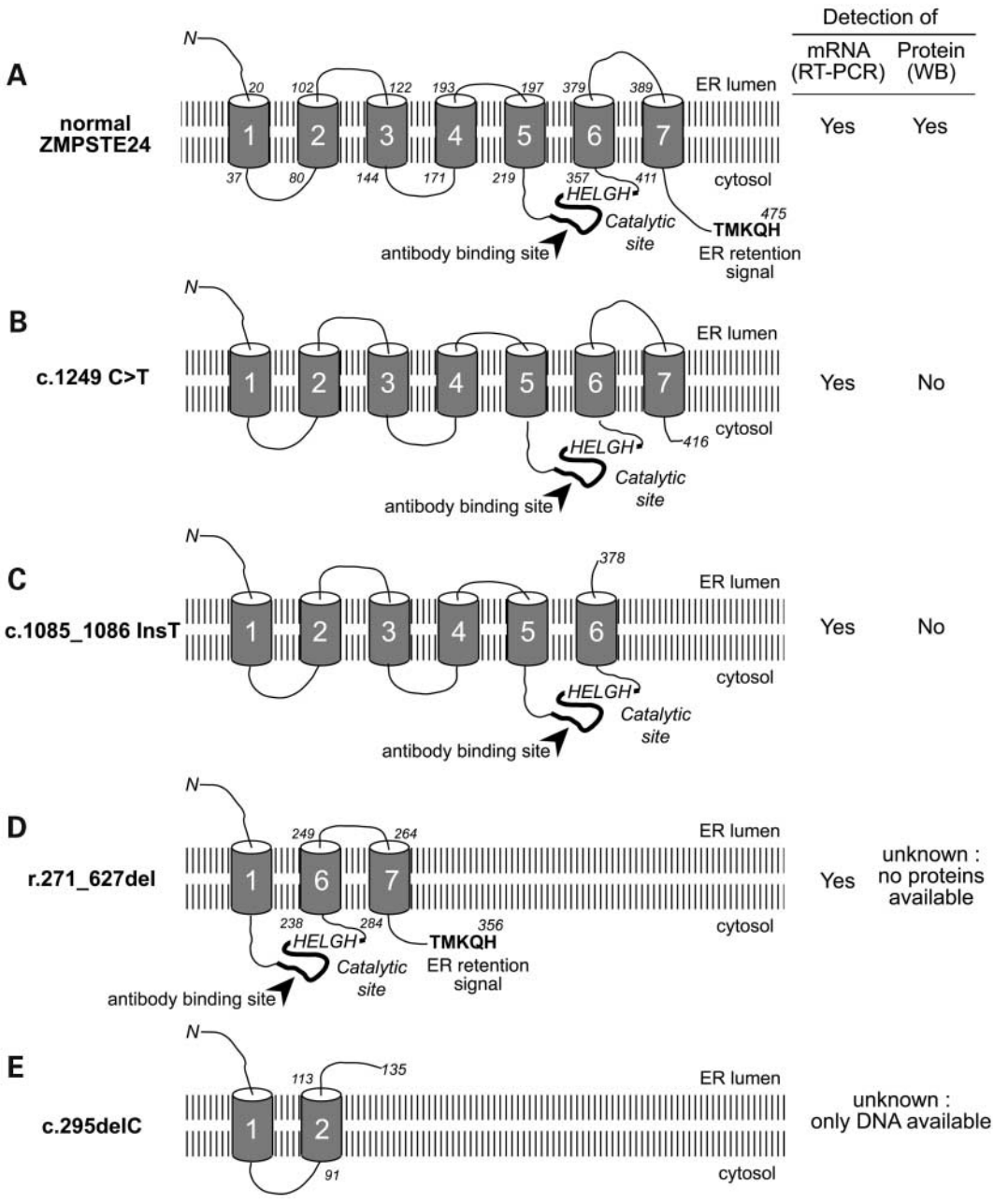

Figure 4. Predicted models of normal and mutated human ZMPSTE24 proteins. For each mutation, experimental detection of mRNAs (RT–PCR) and proteins (western blot) are indicated in the two columns on the right. (**A**) Normal ZMPSTE24 contains seven transmembrane domains as predicted by TMPred and TMHMM algorithms. The zinc metalloprotease catalytic site (HELGH) is included in the binding site (thick line) of the antibody used in western blots. ZMPSTE24 C-terminal ER retention motif TMKQH (KKXX type motif) is also marked. (**B** and **C**) The c.1249 C>T and the c.1085_1086 Ins T mutations shorten ZMPSTE24: the C-terminal ER retention motif is predicted to be lost but the catalytic site remains. Although detected at mRNA level, the two abnormal proteins cannot be detected by western blot suggesting that they are either not synthesised or rapidly degraded. (**D**) The r.271_627 deletion also shortens ZMPSTE24 but the catalytic site is retained as well as the ER retention motif. The corresponding mRNAs have been detected. Protein samples were not available for analysis. (**E**) The c.295delC mutation leads to a very short predicted protein, lacking the last five transmembrane domains.

Lamin A precursors were observed. However, all the mutations in *ZMPSTE24* were found to be heterozygous and, although they all led to the same frameshift with the creation of a PTC, they were not considered sufficient by themselves to cause the RD phenotype (7). Here, we report a complete loss of ZMPSTE24 protein as causing AR-RD and correlate this loss of function with homozygous or compound heterozygous *ZMPSTE24* defects in 10 patients.

Complete lack of ZMPSTE24 was evidenced in all cases explored. In addition, the use of a more stringent protein extraction protocol permitted to detect the presence of unprocessed Prelamin A in the same patients. This approach also

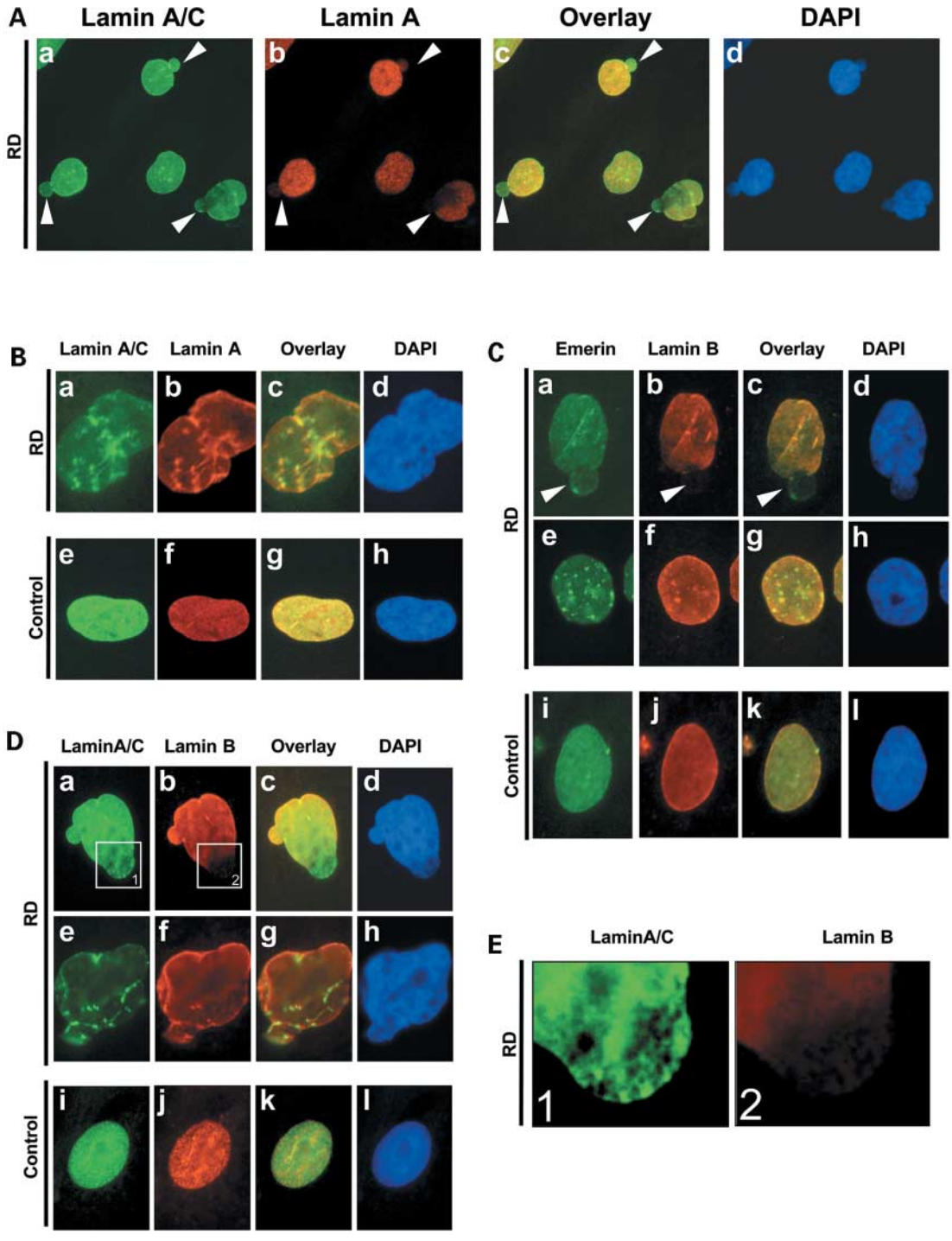

Figure 5. Immunocytochemistry on AR-RD patient fibroblasts. (**A**) Nuclei from RD patients' fibroblasts. (a) Anti-Lamin A/C, (b) anti-Lamin A, (c) overlay and (d) DAPI. Arrows indicate nucleoplasmic blebs stained by anti-Lamin A/C. In AR-RD patients, anti-Lamin A/C antibody detects both Prelamin A and Lamin C, but not Lamin A, as shown by western blot. These same blebs are not stained with anti-Lamin A antibody and thus contain only Lamin C. (**B**) Comparison between nuclei from an AR-RD patient's fibroblasts (a–d) and control fibroblast (e–h). Staining with anti-Lamin A/C (a and e), anti-Lamin A (b and f), overlay (c and g) and DAPI (d and h). The heterogeneous labelling observed in the overlay picture, shows aggregates of both Prelamin A and Lamin C. Control fibroblasts contain homogeneously scattered mature Lamins A and C. (**C**) Nuclei from RD patients (a–h) compared with control (i–l), stained with anti-Emerin (a, e and i) and anti-Lamin B1 (b, f and j), overlay (c, g and k) and DAPI (d, h and l). One bleb with Emerin staining but not Lamin B1 (a, b and c) and aggregates (e, f and g). (**D**) Single nuclei from AR-RD patient fibroblasts (a–h) compared with controls (i–l), stained with anti-Lamin A/C (a, e and i) and anti-Lamin B1 (b, f and j), overlay (c, g and k) and DAPI (d, h and l). Absence of Lamin B1 staining is observed at one nuclear pole (b) whereas it is labelled with anti-Lamin A/C (a). A non-homogeneous labelling is observed (e and f). (**E**) White boxes are enlarged. Boxes 1 and 2 from figure (D) are enlarged and accentuated. Honeycomb structure is evidenced at one nuclear pole with anti-Lamin A/C (1) but is unlabelled with anti-Lamin B1 staining (2).

allowed us to confirm our previous findings, i.e. the absence of mature Lamin A and the presence of Lamin C at normal levels (7). These results indicate that the loss of ZMPSTE24 is the direct cause of Prelamin A accumulation, as Prelamin A cannot be processed by any other cellular proteinase in human or in mice (9,10).

In our previous study, Prelamin A was detected at very low levels, probably as a consequence of inefficient disruption of specific Prelamin A interactions (26). A more stringent step of sonication has been added to the protein extraction protocol, allowing the detection of Prelamin A in all cases. The fact that full-length Prelamin A was observed in RD patients, strongly suggested that the main molecular defects involved in this devastating disorder are loss of function mutations that completely inactivate *ZMPSTE24*, rather than a digenic inheritance of AR-RD as previously proposed (7). To date, two different disease-causing mutations have been reported in *ZMPSTE24*, either in MAD or in RD. It is, however, intriguing that the c.1085_1086insT mutation is shared by the seven RD patients and the unique MAD patient reported (7,20). In MAD, the second associated mutation is a missense substitution (Trp340Arg) that maintains partial ZMPSTE24 enzymatic activity (20). As RD is associated with more dramatic developmental defects leading to neonatal death, null *ZMPSTE24* mutations were expected to be found in these cases. Indeed, a combined transcriptional and genomic approach allowed to identify the inactivating mutations of both *ZMPSTE24* alleles in all the 10 RD patients collected. All patients carried the c.1085_1086InsT insertion, seven at the homozygous state and three at heterozygous state. In one of the three latter cases, we identified a large (5.428 kb) genomic deletion as a second mutation. This genomic deletion leads to the in-frame skipping of exons 3, 4 and 5 at the mRNA level (r.271_627del) with a predicted removal of the second to fifth ZMPSTE24 transmembrane domains. The catalytic motif is maintained at the cytoplasmic side, as well as the C-terminal endoplasmic reticulum (ER) retention motif (TMKQH) (27). However, tissues and proteins were not longer available for this patient, making it impossible to demonstrate whether a truncated ZMPSTE24 polypeptide is present (Fig. 4). In the two other RD patients carrying a heterozygous c.1085_1086insT insertion, second mutations were identified in exons 10 and 3 of the gene. Both were predicted to introduce a PTC due to a nonsense mutation in P10 (c.1249C > T leading to p.Gln417X) and a frameshift cytosine deletion in exon 3 in P12 (c.295delC leading to p.Pro99LeufsX38). The c.1249C > T maps to exon 10 and is predicted to shorten the C-terminal cytoplasmic domain thus removing the TMKQH tetrapeptide corresponding to the ER retention motif (27). This abnormal protein, predicted to be mislocalized, is actually not produced or is degraded as indicated by western blot studies (Fig. 4). The c.295delC is predicted to have an even more deleterious effect as it introduces a PTC in the amino-terminal part, within the second transmembrane domain of the protein, thus removing the last five transmembrane domains as well as the zinc metalloprotease catalytic motif (HEXXH) (Fig. 4). This latter mutation is undoubtedly pathogenic, although only DNA was available for P12.

It has been demonstrated that the PTC occurring in the case of the c.1085_1086insT mutation was associated with the loss of ZMPSTE24 enzymatic activity, even though it is located 3′ to the catalytic domain (20). In addition, the present study demonstrates the complete absence of normal or truncated ZMPSTE24 associated with the c.1085_1086insT (L362fsX18) mutation. For the remaining seven patients affected with RD, the use of several combined molecular methods, i.e. cloning, fluorescent PCR and direct high fidelity sequencing, demonstrated the homozygous c.1085_1086insT status of these patients.

When available, parents from affected cases were explored and found heterozygous for the (T)10 allele. In addition, our analyses revealed that this mutant (T)10 allele is unstable. This instability appears to give rise to a pseudo-frameshift sequencing pattern in homozygous patients. Mononucleotide sequences have been reported, in different genes, as being a preferential target for microsatellite instability (MSI) (28–30). When located in coding regions, MSI may generate frameshift alterations (30). Our observation of a MSI in *ZMPSTE24* is of particular interest. Indeed, this same stretch of thymines in *ZMPSTE24* exon 9 has previously been shown to be a specific target for MSI in case of colorectal tumors with a mutation rate of 8.1% (31). Most of the *ZMPSTE24* mutations involve the same mechanism of a thymine insertion in a known region of MSI, and we thus consider them to be identical mutations at a ‘hotspot’ rather than descendants of a founder allele. In addition, none of the AR-RD patients explored in the present study has consanguineous parents although, in three families, clinical recurrence of the syndrome was reported.

LMNA mutations have been associated with a wide spectrum of distinct tissue specific or systemic disorders (21), whereas *ZMPSTE24* defects have been associated with MAD and RD (7,20). These phenotypes are characterized by clinical features reminiscent of HGPS (reviewed in 22,23) and belong to the *LMNA* mutational spectrum as they affect the Lamin A specific C-terminal globular domain. In particular, *LMNA* mutations observed in typical HGPS and RD result in a splicing defect that removes the second ZMPSTE24-specific recognition and cleavage motif from Lamin A (5–7). As a consequence, ZMPSTE24 is unable to cleave the truncated Prelamin A which persists within the nucleus where it has a toxic effect, leading to nuclear defects whose severity increases during cell divisions (32). This observation is consistent with both our results and observations from *Zmpste24*−/− knock-out mice which are unable to produce the mature Lamin A isoform, whereas normal length Lamin A precursors accumulate and are associated with major nuclear disorganization (9,10). Both knock-out studies reported severe phenotypes in ‘null’ *Zmpste24*−/− mice, closely resembling human Laminopathies and Progeroid disorders.

In RD patients, normal length Lamin A precursors accumulate in nucleoplasmic foci and, as in Progeria, are suspected to have a toxic effect on the cells. Recently, on the basis of double knock-out *Lmna*+/− *Zmpste24*−/− mice, it has been shown that decreasing Prelamin A synthesis prevents the appearance of the progeroid phenotype seen in *Zmpste24*−/− mice (19).

Prelamin A is never observed in controls, because it is immediately processed to mature Lamin A. In RD as well as

in HGPS patients, Prelamin A is produced either at a normal length in the cases of *ZMPSTE24* loss of function mutations or truncated in the cases of *LMNA* cryptic splice-site activation in HGPS (5,6). Normal Prelamin A contains a CaaX-terminal motif, which is a specific target for farnesyl transferase (33), farnesylation being a prerequisite for the first aaX cleavage by ZMPSTE24. Although Prelamin A is farnesylated, removal of the farnesylated aaX cannot occur in AR-RD patients, because of the absence of ZMPSTE24. In the case of *LMNA*-associated HGPS or RD, a truncated Prelamin A is produced, lacking the second ZMPSTE24 post-translational cleavage site (7,32). Therefore, according to the known mechanism of ZMPSTE24 cleavage, truncated Prelamin A is also predicted to remain farnesylated.

On the basis of these results, as the accumulation of normal or truncated Prelamin A is a shared feature in both RD and Progeria, as well as in animal KO models, we hypothesize that the persistence of the farnesylated form might play a key role in the toxic effect of Prelamin A accumulation. If this is the case, variable levels of farnyselated Prelamin A should be directly correlated to the phenotype severity, regardless of the Prelamin A size. From this perspective, it is not surprising that AR-RD patients develop such a dramatic phenotype. Indeed, they can be considered as human *ZMPSTE24* knock-outs, with the highest level of farnesylated Prelamin A ever detected in human cells together with a complete absence of mature Lamin A. Reducing the accumulation of farnyselated Prelamin A could thus open possible avenues towards developing therapeutic approaches in Progeria and related disorders. Finally, as an immediate application of our study, molecular diagnosis may be proposed to RD families who will thus benefit from improved genetic counselling and early prenatal diagnosis of this devastating disorder.

MATERIALS AND METHODS

Patients and samples

Seven patients who were previously reported affected with RD (MIM no. 275210) from six families were included in this study, in addition to three new cases: two from the Netherlands and one from Italy. Fibroblasts cultures were obtained from the first two, from a skin biopsy, and were cultured in DMEM medium containing 10% fetal calf serum, 2 mM L-glutamine and 100 U/ml penicillin–streptomycin (GIBCO BRL).

Western blots

Cultured fibroblasts from patients were trypsinized, pelleted and lysed in 300 μl of 1% Triton X-100, 0.1% SDS, 0.5% sodium deoxycholate, 150 mM NaCl, 1 mM EDTA, 1× protease inhibitors, 1 mM Na_3VO_4 and 1 mM PMSF. Cell extracts were sonicated three times during 30 s and centrifuged 10 min at 10 000 rpm and 4°C. In total protein, 50 μg from each extract were separated in 12% SDS–PAGE gels and transferred to Hybond-ECL nitrocellulose membranes (Amersham). Blots were blocked for 1 h at room temperature in 5% non-fat milk in PT (1× PBS, 1% Tween-20). Afterwards, blots were incubated over night at 4°C with anti-FACE-1 (205-8C10, Daiichi Chemical) or anti-Lamin A/C (sc-7292, Santa Cruz) monoclonal antibodies diluted 1/500 in 3% non-fat milk in PT. Thereafter, blots were washed in PT and incubated for 1 h at room temperature with peroxidase-conjugated goat anti-mouse antibody diluted 1/25 000 in 1.5% non-fat milk in PT. Blots were then washed in PT and incubated with Supersignal West Femto® (for anti-FACE-1) or Pico® (for anti-Lamin A/C) Chemiluminescent Substrates (Pierce) for signal detection.

Genomic and transcriptional analysis

Genomic DNA was extracted from peripheral blood lymphocytes by standard procedures. RNA extraction was performed from fibroblasts cultures by using TRIZOL (Invitrogen-Life Technologies). Reverse transcription was performed with a Superscript II reverse transcriptase (Invitrogen-Life Technologies) following the recommendations of the manufacturer. *ZMPSTE24* coding sequence is available at http://genome.ucsc.edu/. Different oligonucleotide pairs were used to amplify large parts or full-length *ZMPSTE24* transcripts from patients. In Figure 2A, the following RT–PCR primers were used: forward ocn149, 5′-AAAACTCGAGCCATGGGGATGTGGGCAT-3′ and reverse ocn60, 5′-TCCTCCTGGATGTCTTTGTTT-3′. Primer sequences used to amplify and sequence the large genomic deletion in patient P4 (Fig. 3B) are as following: forward int2F2, 5′-ATTGGGAATTGGCTGAAAGA-3′ and reverse ocn48, 5′-TTTCTTATCCCCAGGTAGCC-3′.

Sequencing reactions were performed with a dye terminator procedure and loaded on a CEQ™ 8000 multi-capillary automatic sequencer (Beckman Coulter) according to the manufacturer's recommendations. They were controlled by using a different dye terminator procedure and loaded on ABI capillary automatic sequencer (Applera—ABI3100) according to the procedures of the manufacturer. All sequence variations are described according to den Dunnen recommendations at http://www.hgvs.org/mutnomen. Primers to amplify genomic sequences were located in the flanking introns and were designed as following for exon 3: forward ocn41, 5′-TGTCCTTTCTTTCTTTATACCATGC-3′ and reverse ocn42, 5′-TTAGTGGAAAGCCTGCCAAG-3′; for exon 9: forward ocn53, 5′-CCCATAGTGAAATCAGCTTG G-3′ and reverse ocn54: 5′-TTGAAGCAGGCAAGAGCAT A-3′; for exon 10: forward ocn112, 5′-TTCTTTTGTCCTGCC ATTCC-3′ and reverse ocn113, 5′-GCTTCAAAATTCATT CAGTGTTTT-3′. Most PCR reactions performed in this study were performed in standard conditions using a recombinant Taq DNA polymerase (Invitrogen). Only the PCR reactions to amplify genomic DNA from exon 9 used for direct sequencing and cloning, were performed by using Accuprime Taq DNA polymerase high fidelity (Invitrogen). All primer sequences are listed in Supplemental Material, Table S1 and are available on request.

Fluorescent PCR analysis

Ocn53 was 5′ labelled by fluorochrome D2 (Proligo) and used in combination with ocn54 to amplify and analyse the exon 9 fragment's size. PCR products were mixed with D1 fluorescent size marker, loaded and analysed on CEQ8000

multi-capillary automatic sequencer (Beckman Coulter) according to the recommendations of the manufacturer.

Cloning

Exon 9 from all RD patients and parents available were PCR amplified using AccuPrim Kit (Invitrogen) and inserted into PGEM-T vector (Promega) according the manufacturer's protocol. Bacterial strain XL1blue was transformed with the generated constructs, plated on Agar/LB containing X-gal, IPTG, Ampicilline and incubated overnight at 37°C. Direct PCR reactions were performed on the white colonies which were sequenced by using SP6 and T7 primers included in PGEM-T vector's arms.

In silico analysis

Prediction of sorting signals for mutated ZMPSTE24 proteins were performed using PSORT II web site (http://psort.ims.u-tokyo.ac.jp). The topology of normal and mutated ZMPSTE24 proteins were analysed using the algorithms proposed at TMPred (http://www.ch.embnet.org/software/TMPRED_form.html) and TMHMM (http://www.cbs.dtu.dk/services/TMHMM-2.0/). Both servers indicated similar results regarding the number and the localization of ZMPSTE24 transmembrane domains.

Immunohistochemistry

Immunological and image analyses methods were previously described (7). Primary antibodies were anti-Lamin A/C monoclonal antibody (Clone 4A7) and anti-Emerin (MANEM 8) both provided by Dr G. Morris; anti-Lamin A (provided by Y. Hayashi); anti-Lamin B1 (Sc-6217, Santa Cruz Biotechnologies, Santa Cruz, CA, USA).

SUPPLEMENTARY MATERIAL

Supplementary Material is available at HMG Online.

ACKNOWLEDGEMENTS

We thank the members of the families for their invaluable contribution to this study. The following physicians have to be greatly acknowledged for taking care of the patients and families and providing us with information and samples: Drs Henk Sillevis-Smitt, Elizabeth Flori, Nicole Laurent, Ton Van essen and A.P. Oranje. Drs G. Morris and Y. Hayashi are acknowledged for providing us with antibodies, and André Navarro as managing the cell and DNA core facility of Marseille. We are extremely grateful to Mike Mitchell for critical reading of this manuscript, helpful comments and discussions. This study was supported by a grant from the 'Association Française contre les Myopathies' (AFM), the Institut National de la Santé et de la Recherche Médicale (INSERM), the Assistance Publique des Hôpitaux de Marseille (AP-HM), European Union, CICYT-Spain and Fundación La Caixa (to CL-O) and the Association Méditerranéenne pour la Recherche en Génétique (AMRG). C.L.N. is supported by a fellowship grant from the AFM.

Conflict of Interest statement. None declared.

REFERENCES

1. Witt, D.R., Hayden, M.R., Holbrook, K.A., Dale, B.A., Baldwin, V.J. and Taylor, G.P. (1986) Restrictive dermopathy: a newly recognized autosomal recessive skin dysplasia. *Am. J. Med. Genet.*, **24**, 631–648.
2. Verloes, A., Mulliez, N., Gonzales, M., Laloux, F., Hermanns-Le, T., Pierard, G.E. and Koulischer, L. (1992) Restrictive dermopathy, a lethal form of arthrogryposis multiplex with skin and bone dysplasia: three new cases and review of the literature. *Am. J. Med. Genet.*, **43**, 539–547.
3. Lenz, W. and Meschede, D. (1993) Historical note on restrictive dermopathy and report of two new cases. *Am. J. Med. Genet.*, **47**, 1235–1237.
4. Mau, U., Kendziorra, H., Kaiser, P. and Enders, H. (1997) Restrictive dermopathy: report and review. *Am. J. Med. Genet.*, **71**, 179–185.
5. De Sandre-Giovannoli, A., Bernard, R., Cau, P., Navarro, C., Amiel, J., Boccaccio, I., Lyonnet, S., Stewart, C.L., Munnich, A., Le Merrer, M. *et al.* (2003) Lamin A truncation in Hutchinson–Gilford progeria. *Science*, **300**, 2055.
6. Eriksson, M., Brown, W.T., Gordon, L.B., Glynn, M.W., Singer, J., Scott, L., Erdos, M.R., Robbins, C.M., Moses, T.Y., Berglund, P. *et al.* (2003) Recurrent *de novo* point mutations in lamin A cause Hutchinson–Gilford progeria syndrome. *Nature*, **423**, 293–298.
7. Navarro, C., De Sandre-Giovannoli, A., Bernard, R., Boccaccio, I., Boyer, A., Genevieve, D., Hadj-Rabia, S., Gaudy-Marqueste, C., Smith, H.S., Vabres, P. *et al.* (2004) Lamin A and ZMPSTE24 (FACE-1) defects cause nuclear disorganisation and identify restrictive dermopathy as a lethal neonatal laminopathy. *Hum. Mol. Genet.*, **13**, 2493–2503.
8. Freije, J.M., Blay, P., Pendas, A.M., Cadinanos, J., Crespo, P. and Lopez-Otin, C. (1999) Identification and chromosomal location of two human genes encoding enzymes potentially involved in proteolytic maturation of farnesylated proteins. *Genomics*, **58**, 270–280.
9. Pendas, A.M., Zhou, Z., Cadinanos, J., Freije, J.M., Wang, J., Hultenby, K., Astudillo, A., Wernerson, A., Rodriguez, F., Tryggvason, K. *et al.* (2002) Defective prelamin A processing and muscular and adipocyte alterations in Zmpste24 metalloproteinase-deficient mice. *Nat. Genet.*, **31**, 94–99.
10. Bergo, M.O., Gavino, B., Ross, J., Schmidt, W.K., Hong, C., Kendall, L.V., Mohr, A., Meta, M., Genant, H., Jiang, Y. *et al.* (2002) Zmpste24 deficiency in mice causes spontaneous bone fractures, muscle weakness, and a prelamin A processing defect. *Proc. Natl Acad. Sci. USA*, **99**, 13049–13054.
11. Corrigan, D.P., Kuszczak, D., Rusinol, A.E., Thewke, D.P., Hrycyna, C.A., Michaelis, S. and Sinensky, M.S. (2005) Prelamin A endoproteolytic processing *in vitro* by recombinant Zmpste24. *Biochem. J.*, **387 (pt 1)**, 129–138.
12. Hutchison, C.J. and Worman, H.J. (2004) A-type lamins: guardians of the soma? *Nat. Cell Biol.*, **6**, 1062–1067.
13. Fawcett, D. (1966) On the occurrence of a fibrous lamina on the inner aspect of the nuclear envelope in certain cells of vertebrates. *Am. J. Anat.*, **119**, 129–145.
14. Bridger, J.M., Kill, I.R., O'Farrell, M. and Hutchison, C.J. (1993) Internal lamin structures within G1 nuclei of human dermal fibroblasts. *J. Cell Sci.*, **104** (Pt 2), 297–306.
15. Hozak, P., Sasseville, A.M., Raymond, Y. and Cook, P.R. (1995) Lamin proteins form an internal nucleoskeleton as well as a peripheral lamina in human cells. *J. Cell Sci.*, **108** (Pt 2), 635–644.
16. Shumaker, D.K., Kuczmarski, E.R. and Goldman, R.D. (2003) The nucleoskeleton: lamins and actin are major players in essential nuclear functions. *Curr. Opin. Cell Biol.*, **15**, 358–366.
17. Beck, L.A., Hosick, T.J. and Sinensky, M. (1990) Isoprenylation is required for the processing of the lamin A precursor. *J. Cell Biol.*, **110**, 1489–1499.
18. Sinensky, M., Fantle, K., Trujillo, M., McLain, T., Kupfer, A. and Dalton, M. (1994) The processing pathway of prelamin A. *J. Cell Sci.*, **107** (Pt 1), 61–67.
19. Fong, L.G., Ng, J.K., Meta, M., Cote, N., Yang, S.H., Stewart, C.L., Sullivan, T., Burghardt, A., Majumdar, S., Reue, K. *et al.* (2004) Heterozygosity for Lmna deficiency eliminates the progeria-like phenotypes in Zmpste24-deficient mice. *Proc. Natl Acad. Sci. USA*, **101**, 18111–18116.
20. Agarwal, A.K., Fryns, J.P., Auchus, R.J. and Garg, A. (2003) Zinc metalloproteinase, ZMPSTE24, is mutated in mandibuloacral dysplasia. *Hum. Mol. Genet.*, **12**, 1995–2001.

21. Mounkes, L., Kozlov, S., Burke, B. and Stewart, C.L. (2003) The laminopathies: nuclear structure meets disease. *Curr. Opin. Genet. Dev.*, **13**, 223–230.
22. Mounkes, L.C. and Stewart, C.L. (2004) Aging and nuclear organization: lamins and progeria. *Curr. Opin. Cell Biol.*, **16**, 322–327.
23. Novelli, G. and D'Apice, M.R. (2003) The strange case of the 'lumper' lamin A/C gene and human premature ageing. *Trends Mol. Med.*, **9**, 370–375.
24. Happle, R., Stekhoven, J.H., Hamel, B.C., Kollee, L.A., Nijhuis, J.G., Anton-Lamprecht, I. and Steijlen, P.M. (1992) Restrictive dermopathy in two brothers. *Arch. Dermatol.*, **128**, 232–235.
25. Smitt, J.H., van Asperen, C.J., Niessen, C.M., Beemer, F.A., van Essen, A.J., Hulsmans, R.F., Oranje, A.P., Steijlen, P.M., Wesby-van Swaay, E., Tamminga, P. *et al.* (1998) Restrictive dermopathy. Report of 12 cases. Dutch Task Force on Genodermatology. *Arch. Dermatol.*, **134**, 577–579.
26. Barton, R.M. and Worman, H.J. (1999) Prenylated prelamin A interacts with Narf, a novel nuclear protein. *J. Biol. Chem.*, **274**, 30008–30018.
27. Teasdale, R.D. and Jackson, M.R. (1996) Signal-mediated sorting of membrane proteins between the endoplasmic reticulum and the golgi apparatus. *Annu. Rev. Cell Dev. Biol.*, **12**, 27–54.
28. Zirvi, M., Nakayama, T., Newman, G., McCaffrey, T., Paty, P. and Barany, F. (1999) Ligase-based detection of mononucleotide repeat sequences. *Nucleic Acids Res.*, **27**, e40.
29. de Leeuw, W.J., van Puijenbroek, M., Merx, R., Wijnen, J.T., Brocker-Vriends, A.H., Tops, C., Vasen, H., Cornelisse, C.J. and Morreau, H. (2001) Bias in detection of instability of the (C)8 mononucleotide repeat of MSH6 in tumours from HNPCC patients. *Oncogene*, **20**, 6241–6244.
30. Paoloni-Giacobino, A., Rey-Berthod, C., Couturier, A., Antonarakis, S.E. and Hutter, P. (2002) Differential rates of frameshift alterations in four repeat sequences of hereditary nonpolyposis colorectal cancer tumors. *Hum. Genet.*, **111**, 284–289.
31. Mori, Y., Yin, J., Rashid, A., Leggett, B.A., Young, J., Simms, J., Kuehl, P.M., Langenberg, P., Meltzer, S.J. and Stine, O.C. (2001) Instabilotyping: comprehensive identification of frameshift mutations caused by coding region microsatellite instability. *Cancer Res.*, **61**, 6046–6049.
32. Goldman, R.D., Shumaker, D.K., Erdos, M.R., Eriksson, M., Goldman, A.E., Gordon, L.B., Gruenbaum, Y., Khuon, S., Mendez, M., Varga, R. *et al.* (2004) Accumulation of mutant lamin A causes progressive changes in nuclear architecture in Hutchinson–Gilford progeria syndrome. *Proc. Natl Acad. Sci. USA*, **101**, 8963–8968.
33. Roskoski, R., Jr (2003) Protein prenylation: a pivotal posttranslational process. *Biochem. Biophys. Res. Commun.*, **303**, 1–7.